Diffraction Efficiency of Thin Film Holographic Beam Steering Devices

Charles M. Titus
Kent State University, Kent, Ohio

John Pouch, Hung Nguyen, and Felix Miranda
Glenn Research Center, Cleveland, Ohio

Philip J. Bos
Kent State University, Kent, Ohio

Since its founding, NASA has been dedicated to the advancement of aeronautics and space science. The NASA Scientific and Technical Information (STI) Program Office plays a key part in helping NASA maintain this important role.

The NASA STI Program Office is operated by Langley Research Center, the Lead Center for NASA's scientific and technical information. The NASA STI Program Office provides access to the NASA STI Database, the largest collection of aeronautical and space science STI in the world. The Program Office is also NASA's institutional mechanism for disseminating the results of its research and development activities. These results are published by NASA in the NASA STI Report Series, which includes the following report types:

- TECHNICAL PUBLICATION. Reports of completed research or a major significant phase of research that present the results of NASA programs and include extensive data or theoretical analysis. Includes compilations of significant scientific and technical data and information deemed to be of continuing reference value. NASA's counterpart of peer-reviewed formal professional papers but has less stringent limitations on manuscript length and extent of graphic presentations.

- TECHNICAL MEMORANDUM. Scientific and technical findings that are preliminary or of specialized interest, e.g., quick release reports, working papers, and bibliographies that contain minimal annotation. Does not contain extensive analysis.

- CONTRACTOR REPORT. Scientific and technical findings by NASA-sponsored contractors and grantees.

- CONFERENCE PUBLICATION. Collected papers from scientific and technical conferences, symposia, seminars, or other meetings sponsored or cosponsored by NASA.

- SPECIAL PUBLICATION. Scientific, technical, or historical information from NASA programs, projects, and missions, often concerned with subjects having substantial public interest.

- TECHNICAL TRANSLATION. English-language translations of foreign scientific and technical material pertinent to NASA's mission.

Specialized services that complement the STI Program Office's diverse offerings include creating custom thesauri, building customized databases, organizing and publishing research results . . . even providing videos.

For more information about the NASA STI Program Office, see the following:

- Access the NASA STI Program Home Page at *http://www.sti.nasa.gov*

- E-mail your question via the Internet to help@sti.nasa.gov

- Fax your question to the NASA Access Help Desk at 301–621–0134

- Telephone the NASA Access Help Desk at 301–621–0390

- Write to:
  NASA Access Help Desk
  NASA Center for AeroSpace Information
  7121 Standard Drive
  Hanover, MD 21076

NASA/TM—2003-211806

Diffraction Efficiency of Thin Film Holographic Beam Steering Devices

Charles M. Titus
Kent State University, Kent, Ohio

John Pouch, Hung Nguyen, and Felix Miranda
Glenn Research Center, Cleveland, Ohio

Philip J. Bos
Kent State University, Kent, Ohio

National Aeronautics and
Space Administration

Glenn Research Center

February 2003

Available from

NASA Center for Aerospace Information
7121 Standard Drive
Hanover, MD 21076

National Technical Information Service
5285 Port Royal Road
Springfield, VA 22100

Available electronically at http://gltrs.grc.nasa.gov

DIFFRACTION EFFICIENCY OF THIN FILM HOLOGRAPHIC BEAM STEERING DEVICES

Charles M. Titus
Kent State University
Kent, Ohio 44242

John Pouch, Hung Nguyen, and Felix Miranda
National Aeronautics and Space Administration
Glenn Research Center
Cleveland, Ohio 44135

Philip J. Bos
Kent State University
Kent, Ohio 44242

Abstract

Dynamic holography has been demonstrated as a method for correcting aberrations in space deployable optics, and can also be used to achieve high-resolution beam steering in the same environment. In this paper, we consider some of the factors affecting the efficiency of these devices. Specifically, the effect on the efficiency of a highly collimated beam from the number of discrete phase steps per period is considered for a blazed thin film beam steering grating. The effect of the number of discrete phase steps per period on steering resolution is also considered. We also present some result of Finite-Difference Time-Domain (FDTD) calculations of light propagating through liquid crystal "blazed" gratings. Liquid crystal gratings are shown to spatially modulate both the phase and amplitude of the propagating light.

1. Introduction

As NASA develops a need to transmit greater amounts of data over long distances, there is a need to develop new technologies capable of such performance.[1,2] Current S- and X-band RF technology provides only limited room for increasing the data communication rate.[2,3] The use of K_a-band technology may increase the usable photon flux by a few orders of magnitude, but even that may not be enough to permit, for example, high-speed, long-distance communication of high-resolution image data.[4] In addition, increasing the RF transmitter power level does not get past the bandwidth limitations of the carrier frequency. For that reason, NASA is exploring the use of shorter wavelengths in the near IR, where the greater directivity of transmitting beams can increase the photon flux and bandwidth.

However, this potential benefit is not without cost, for it involves trading problems with existing RF technology for a new set of problems. Among these new problems is the necessity for some means of high-resolution optical beam steering in order to maintain connection of the more directional signal beam with the distant receiver. Because of the anticipated demand for higher data rates at all transmission distances, special steps must be taken in order to ensure a high signal concentration at the receiving end. In order to maintain the intensity of a propagating laser beam after long propagation distances, the beam must possess a divergence of a few microradians or less. Along with this directivity requirement comes the need for a steering capability of even greater accuracy, i.e., sub-microradian beam pointing technology.[5]

The most mature beam steering devices achieve deflection through mechanical means. Although mechanical pointing technology is being considered for use in deep-space optical communications,[5–7] such devices may not provide the needed precision.

Liquid crystal devices have already been considered for use in beam steering applications,[8-10] as well as for the closely related function of tip-tilt correction of wave fronts.[11]

In this paper we discuss factors influencing the range, resolution, and number of steering angles available from a "phase-only" liquid crystal spatial light modulator (LC-SLM). Computational simulations are used to quantify the effect of phase stair-stepping on beam steering (i.e., diffractive) performance. Simulation data is also presented to quantify the impact of beam truncation by the diffracting aperture and surface flatness.

These devices can be designed at or between either of two extremes: large pixels producing stair-stepped phase modulation or small pixels whose director distortions produce smoothed phase profiles. Here, we discuss the large pixel variety. The effects of director distortion and finite cell thickness will be considered in later publications.

2. Background

The LC-SLM consists of two glass plates sandwiching a thin (~10 μm or less) layer of liquid crystalline material. One substrate is coated with a single common electrode, usually held at zero volts. The other glass substrate is patterned with a number of uniformly sized and spaced discrete electrodes.

If suitably addressed, the electrodes of the LC-SLM selectively reorient the liquid crystal to form a one-dimensional phase grating. This grating is used to impose a periodic "blazed" phase profile onto the incident light (fig. 1). In beam steering or tilt-tip correction applications, the goal is to provide the equivalent of a linear phase ramp with its 2π phase degeneracies removed (fig. 2). Operated in this fashion, the LC-SLM can be used as a means of redirecting the path of monochromatic light in one dimension. Two-dimensional beam steering or tip-tilt correction can be obtained by either cascading two one-dimensional LC-SLM's, or by encoding onto a single device a two-dimensional array of individually addressable electrodes.

The use of an LC-SLM in this manner has carried the label of Optical Phased Array (OPA) technology.[8,9] In one implementation of liquid crystal OPA technology,[10] every n^{th} electrode is linked together in order to reduce the number of off-device connections. This approach is taken primarily to make more practical the fabrication of large apertures containing a large number of electrodes. However, that approach also limits available steering angles to a discrete number of angularly separated deflections. In order to completely cover an entire region of interest, cascading with a second fine-tuning stage is required. Technology does exist for connecting and *individually* addressing each of a moderately large number of (more than one thousand) electrodes. This latter form of LC-OPA technology is the subject of this paper.

Prior analysis of the OPA, for which identical stair-stepped phase approximations of ideal blaze periods are repeated across the entire device, has yielded a theoretical maximum beam steering efficiency of:[8]

$$\eta = \text{sinc}^2(\pi / N) \tag{1}$$

where N is the number of stair-stepped phase segments in each identical blaze profile. It is assumed that all modulo-2π resets of the original ideal phase profile fall between electrodes. Below we will show that this result extends to the more general case of resets falling anywhere in the LC-SLM, even in the middle of electrodes, if the phase retardation produced by those electrodes is properly chosen. Hence, it is predicted that individually addressable lines will permit continuous steering from this stair-stepped LC-SLM device, without any penalty beyond that imposed by eq. (1). In other words,

this device does not, in theory, possess any pixel-related limit to angular resolution. This potential for achieving continuous steering from liquid crystal OPA technology has not, to our knowledge, been previously analyzed and discussed.

Experimental measurement of the beam steering efficiency of one OPA-like liquid crystal grating was shown to fall short of that predicted by eq. (1).[11] The cause of that discrepancy is one of the motivations for this paper.

As was mentioned, these devices can be implemented at or between two extremes. At one extreme the LC-SLM pixels or stripes (one for each electrode) consist of electrodes large enough that the phase profile exhibits stair-stepping. Fringe fields and liquid crystal elasticity at the edges of the electrodes (i.e., at the boundaries between adjacent pixels or stripes) cause some smoothing of this stair-stepping, but the area occupied by those behaviors is relatively insignificant relative to the much larger area of the electrodes as a whole. As a result, the device exhibits relatively sharp phase "resets," closely approximating that of an "ideal" blazed phase grating (fig. 3a). At the other extreme, the pixels or stripes would be small enough that fringe fields and liquid crystal elasticity completely smooth out the phase profile, preventing the appearance of sharp phase "resets" (fig. 3b). This paper will be restricted to the former extreme.

3. Methodology

Assuming the thin-layer model, diffractive behavior can be obtained by means of a numerical evaluation of an appropriate scalar diffraction integral, such as the Integral Theorem of Helmholtz and Kirchhoff:[12]

$$\psi(\mathbf{r}) = \frac{1}{4\pi} \int \int_S \mathbf{n} \bullet \left[\psi(\mathbf{r}')\nabla' G - G\nabla' \psi(\mathbf{r}') \right] dS' \tag{2}$$

where ψ is a complex scalar field representing light emerging from the grating layer, $\mathbf{r}' = (x',y',z')$ is a location on the exit surface S' of the diffracting object, $\mathbf{r} = (x,y,z)$ is a location of some diffraction observation, $\mathbf{n}$ is the local normal to the surface of the diffracting object, and G is the appropriate Green's function. For a one-dimensional grating such as is central to this discussion, the above equation is easily recast as a line integral:[13]

$$\psi(\mathbf{r}) = -\frac{\exp(-i\pi/4)}{(8k\pi)^{1/2}} \int_{-d}^{d} \frac{\exp(ikR_\parallel)}{R_\parallel^{1/2}} \left[\partial_y \psi(x') + \frac{iky}{R_\parallel} \psi(x') \right] dx' \tag{3}$$

where for a one-dimensional planar diffracting aperture $R_\parallel = |\mathbf{r}-\mathbf{r}'|$, $\mathbf{r} = (x,y,0)$, $\mathbf{r}' = (x',0,0)$, k is the magnitude of the wave vector, and the aperture extends over the range $x \subset [-d,d]$.

The two bracketed terms in eq. (3) are direct descendants of the two Rayleigh-Sommerfeld components of eq. (2). In general, if paraxial calculations are carried out for feature sizes within the aperture and propagation distance both much larger than the wavelength, the two Rayleigh-Sommerfeld components and the Helmholtz-Kirchhoff average of the two do not produce significantly different results, in particular for small deflection angles. The computations in this study evaluate the second term. For a Gaussian profile at the minimum beam waist, that term integrates the one-dimensional profile of the electric field of the layer-processed beam:

$$\psi(x') = E_0 \exp\left[\frac{-(x')^2}{w_0^2} \right] \exp\left[i\phi(x') \right] \tag{4}$$

where w_0 is the minimum beam waist radius and x' is the in-plane distance from the center of the beam. In order to approximate thin layer phase gratings, the phase term, $\exp[i\pi(x')]$ can be tailored to the desired grating profile. For an unhindered Gaussian beam, $\phi(x) = 0$.

Since the application of interest is optical communication to and from deep space probes, it is assumed that the propagation distance $[R_\parallel = |\mathbf{r}\text{-}\mathbf{r'}|$ in eq. (3)] is large enough to qualify the diffractive behavior as "far field" (beyond some propagation distance, the angular dependence of diffraction will be independent of that distance).

All thin-layer approximated scalar diffraction calculations below were performed for a $\lambda = 1~\mu m$ Gaussian beam with a minimum waist of 25 cm coinciding with the "very thin" LC-SLM. All results are presented in the form of Strehl ratios. The Strehl ratio is defined here as the ratio of a particular diffracted intensity (field squared) to the peak intensity of an unhindered beam at the same propagation distance. That reference point was computed using the same Gaussian source, for an aperture diameter equal to $8w_0$. For calculations of the Strehl ratio, in which one intensity is divided by another, the value of E_0 is not important.

4. Results

The above calculation method was utilized to gauge the impact of beam truncation, surface flatness, and phase stair-stepping on the far field diffraction performance of large-pixel LC-SLM's. Since it is desirable to provide the maximum signal intensity to the receiver, it is important to know how each of these factors will influence the design of free-space optical communication components such as the beam-steering LC-SLM.

A. Beam Truncation

It is well known that if an aperture truncates a beam of light directed at it, the aperture not only blocks some of the incident light but also redirects some of the transmitted light into higher diffraction orders. This will also affect the Strehl ratio at the center of the propagating beam. For example, the simulated impact of beam truncation on a 25-cm-waist beam with $\lambda = 1~\mu m$ is shown in fig. 4. If the aperture's width is four times the minimum beam waist (which is assumed to occur in the aperture "plane"), the Strehl ratio measured at the center of the propagating beam in the far field is still a healthy 0.99. If the aperture size is reduced to three times the minimum waist, the Strehl ratio is reduced to 0.94, and if the aperture is further reduced to twice the minimum waist, to 0.72. Such losses would set an upper limit for performance, subject to other sources of loss.

B. Imperfect Optical Surfaces

If an optical surface in a beam steering device is less than perfect, those aberrations also reduce the amount of energy delivered to the intended direction. Optical surface imperfections are commonly decomposed into constituent aberration modes, which are then related to image-related effects. Liquid crystal devices employ "flat" manufactured transmissive and reflective glass substrates whose surfaces are perhaps better represented as a Fourier sum of surface undulation terms, each term of a different spatial frequency. One can then analyze the optical effect of each frequency component and determine which spatial frequency components, and how much of each, can be tolerated. The phase profile of such phase undulations, concave at the center of the aperture diameter, can be described by:

$$\phi(x) = 2\pi A \cos\left[2\pi\left(\frac{x - x_{midpoint}}{D} - 0.5\right)\right] \quad\quad\quad (5)$$

where A is one-half of the peak-to-valley amplitude of the undulation, x is the surface location, $x_{midpoint}$ is the center of the aperture, and D is the width of the aperture. This factor was substituted into eq. (4) to obtain the thin-layer approximation of the field transmitted through or reflected from the surface. For a reflective surface, the phase ϕ in eq. (5) is multiplied by two, accounting for the total optical path offset.

The effect of surface undulations can be computed for the case of light reflected from a nominally flat mirror. Assuming that the mirror size is four times the minimum waist (which coincides with the mirror surface), the effect of a surface undulation whose period equals the aperture size can be seen in fig. 5. Those results were obtained for the case of an undulation centered on the mirror, concave at the center. Even if the peak-to-valley undulation amplitude is a very fine $\lambda/20$, the resulting Strehl ratio at the center of the far field is reduced to 0.94. Performance for larger undulation amplitudes is noticeably worse (fig. 6). As the undulation frequency increases beyond the range of fig. 6, light will continue to be diverted into other diffraction orders until the undulations become smaller than a wavelength, at which point the surface will again appear to be flat.

Of course, a glass or reflective silicon substrate employed in an LC-SLM could possess a range of undulation frequencies resulting from the manufacturing process, so no one spatial frequency will dominate. Nevertheless, it is clear that manufacturing imperfections will play a role and should be considered.

This last point provides reason for concern. If space probes are to be equipped with meter-class optical apertures, it will not likely be feasible to launch glass apertures of thickness sufficient to provide stable, precise optical surfaces. Instead, optical components will likely be of lower mass, and thus not as rigid, and more prone to significant surface imperfections. In order to make use of optical surfaces with substantial imperfections, it may be necessary to perform wavefront correction close to the source of the imperfections. It is not inconceivable that a two-dimensional LC-SLM could provide that function while simultaneously steering the beam.

C. Phase Stair-stepping

We now return to the issue of phase stair-stepping, which is the product of the segmented design of LC-SLM electrodes. As shown in figs. 2 and 3a, the principle behind OPA technology involves removal of 2π degeneracies from a linear phase ramp prescribing the beam deflection angle, and then utilizing that blazed phase profile to assign phase values to the OPA's segments. This process is simple and straightforward if all of the "resets" fall between segments, as shown in fig. 3a. However, as was mentioned earlier, that approach permits only a finite number of discrete deflection angles, thereby placing a limitation on beam steering *angular resolution*.

The angular resolution, as the term is used here, is not the same as the ability of a beam steering device to resolve spots. The maximum number of resolvable spots obtainable from a beam deflecting device has been defined as the device's maximum deflection angle divided by the beam's "diffraction limited angle."[14] For a Gaussian beam that angle is defined as the divergence angle. If a beam steering device is engineered to provide deflection to only those separated angles, it will not be capable of continuously covering each point in its angular range with a signal of uniform intensity (see fig. 7). A device may be capable of resolving the maximum number of spots within its angular range, but unless it can steer to angles between the locations of those spots, its angular resolution is limited to the angle between those spots. In order to permit very high signal intensities everywhere within the device's angular range, angular steering resolution must be finer than spot resolution.

Achieving sub-spot angular resolution (i.e., sub-microradian resolution, for deep space optical communications using meter-class transmitting apertures) may at times require that the original linear

phase ramp produce resets which do not fall between OPA segments (fig. 8). It is important that any such OPA segments produce the appropriate phase retardation level. If the phase of those segments is incorrectly assigned, diffraction performance (i.e., beam steering efficiency) will suffer.

One obvious solution is to assign each of these "interperiod" segments a phase equal to the average value of the ideal blazed phase profile within the segment, as shown in fig. 9. This approach can then be described as applying two operations to the original linear phase ramp, namely modulo-2π and area averaging, in that order. Those two operations can be carried out in reverse order, producing interperiod phase values as shown in fig. 10.

The difference between these two approaches is illustrated in fig. 11. For instance, applying the first approach to a linear phase ramp for which the modulo-2π blaze width is equal to the width of 2 and 1/3 electrode segments, the resulting phase profile will appear as shown in fig. 11a. The phase profile using the second approach appears in fig. 11b. It is only when the blaze width equals an integer number of electrode segments that the stair-stepped phase profile obtained using either approach will produce identical neighboring stair-stepped blazes as are found in fig. 3a.

Diffraction simulations were performed for grating phase profiles obtained using each approach. In each simulation, stair-step segments of 100 μm were used to define the stair-stepped phase profiles covering a 1m wide one-dimensional aperture. Each simulation was carried out over a range of deflection angles, each of which is characterized by its own ideal linear phase ramp. Each linear phase ramp corresponds to a number of electrode segments per ideal blaze period, not necessarily an integer. At each value of electrodes per period, the diffracted intensity at the intended far field deflection angle was divided by that produced by the corresponding unbroken linear phase ramp to produce the Strehl ratio data appearing in fig. 12.

For both methods of obtained stair-stepped phase profiles, the Strehl ratio at integer values of electrodes per period matches that obtained from eq. (1). For non-integer values, the first approach falls well below those values, while the second approach does not. Utilizing the second method, high-resolution steering and tip-tilt correction is possible from the LC-SLM. Performance does begin to falter at and below eight electrodes per period, as has been noted.[8,11] Although it might appear that the "irregular periodicity" (see fig. 11b) of the more desirable second stair-step approach might violate the grating condition of its underlying blazed phase profile, such is not the case. The center of each of the stair-step segments does fall on the underlying linear phase ramp, and on its blazed-phase equivalent.

D. Liquid Crystal Layer Simulations

The diffraction simulations above employ approximations of the fields emerging from thin layer liquid crystal gratings. Those computations do not take into account optical anisotropy and spatial variations of the liquid crystal director required to produce diffraction gratings. In a real device, application of appropriate voltages to the closely spaced electrodes might lead to a director configuration which looks somewhat like fig. 1. In order to increase the level of accuracy of diffraction simulations, one must obtain more accurate surface fields than were utilized above. Direct analytical solution for the influence of such a structure on a propagating beam is at best very difficult. However, numerical methods such as the Finite-Difference Time-Domain (FDTD)[15] are capable of providing a very accurate solution for such a problem. Such analysis may provide insight into the impact of anisotropy and inhomogeneity on diffractive performance.

An illustrative two-dimensional simulation of those effects was conducted for this study. An idealized director configuration (fig. 13) was used as the repeated periodic unit of a hypothetical second-order liquid crystal grating designed to steer to 20 degrees. Segmentation was not encoded into the structure at this point, so as to promote the visibility of anisotropy and inhomogeneity-induced effects. The finite grating consisted of about 200 periods. The near field simulation employed FDTD to obtain the response of the idealized liquid crystal grating to an out-of-plane H polarized incident beam of Gaussian profile.

After obtaining a steady-state computed result, a snapshot was obtained of the fields in and beyond the grating. A section of this snapshot is shown in fig. 14, with the grating periods artificially outlined. While the grating appears to have imparted some deflection onto the transmitted fields, there is some disorganization in those fields, which may indicate reduced diffraction efficiency. The disorganization can be separated into amplitude and phase effects as shown in figs. 15 and 16. It appears from fig. 16 that the "phase-only" grating also modulates the transmitted intensity, which degrades the diffraction efficiency below the amount predicted by some imperfect phase modulation alone.

A more complete study of FDTD simulations of segmented liquid crystal beam steering gratings will be carried out in the near future.

5. Conclusions

Implementation of optical communications with deep space probes will require very precise sub-microradian steering of the communication beam in order to maximize the received power. In addition, the received wavefronts may also require further correction, some component of which may be tip-tilt. We have analyzed the possibility of using liquid crystal spatial light modulators (LC-SLMs) to meet these needs. Three factors influencing the beam steering performance of these segmented liquid crystal devices have been analyzed: beam truncation, surface flatness, and phase stair-stepping.

If transmitting a laser beam through an aperture, any truncation of the beam by the aperture detracts from the intensity arriving at a distant receiver. This effect begins to be noticed for apertures less than four times the waist of the beam passing through the aperture.

It is also important to avoid wavefront distortions resulting from imperfect optical surfaces, such as reflective or transmissive substrates used in the fabrication of the LC-SLM. Analysis shows that imperfections of as little as $\lambda/20$ can impose performance penalties of approximately 5 percent, and much more as the magnitude of surface imperfection grows. If those imperfections cannot be eliminated, wavefront correction is necessary, and the LC-SLM may be capable of performing those corrections.

Further analysis was conducted for one limiting case of the LC-SLM, i.e., electrodes large enough that fringe fields and elastic behavior contribute very little to device performance. In that case, the phase retardation profile produced by an LC-SLM will appear to be stair-stepped. In order to maximize LC-SLM speed and minimize scattering losses, the device should be as thin as possible, which means removing the 2π degeneracies from the phase profile. That step produces phase "resets" in the final stair-stepped phase profile.

It is already known that these resets do carry a penalty, but prior analyses considered only the case in which individual stair-step approximated blaze periods contain fixed and identical numbers of segments. This limits any segmented liquid crystal device to a finite number of discretely separated steering angles. That result has been extended to the more general case of phase resets falling on, and not just between, electrode segments. There is a correct choice for the phase value to be produced at electrodes for which a reset falls within bounds of that electrode. If the phase stair-step is obtained by averaging the value of the underlying blazed phase profile over each electrode before removing the 2π degeneracy, analysis shows that it does not matter where the reset falls. As a result, we can say that continuous beam steering is possible without any added penalty.

As is already known, increasing the steering angle (i.e., blazes of smaller size) or increasing the number of waves being corrected by a given fixed aperture results in increased diffractive losses. Use of eight steps per blaze will result in a theoretical 5 percent loss, measured at the receiver's collecting aperture.

References

1. K. Wilson, "Optical Communications for Deep Space Missions," IEEE Communications **38**, 8, 134–139 (2000).
2. C.D. Edwards, C.T. Stelzried, L.J. Deutsch, and L. Swanson, "NASA's Deep-Space Telecommunications Road Map," TMO Progress Report **42-136**, Jet Propulsion Laboratory, Pasadena CA, 1–20 (1999).
3. C. Chen, J.W. Alexander, H. Hemmati, S. Monacos, T. Yan, S. Lee, J.R. Lesh, and S. Zingales, "System Requirements for a Deep Space Optical Transceiver," SPIE Proc. **3615**, 142–152 (1999).
4. H. Hemmati, K. Wilson, M. Sue, L. Harcke, M. Wilhelm, C. Chen, J. Lesh, and Y. Feria, "Comparative Study of Optical and Radio-Frequency Communication Systems for a Deep-Space Mission," TDA Progress Report **42–128**, Jet Propulsion Laboratory, Pasadena CA, 1–33 (1997).
5. S. Lee, J.W. Alexander, and G.G. Ortiz, "Sub-Microradian Pointing System Design for Deep-Space Optical Communication," in *Free-Space Laser Communication Technologies XIII*, G. Stephen Mecherle, ed., Proc. SPIE **4272**, 104–111 (2001).
6. J.W. Alexander, S. Lee, and C. Chen, "Pointing and Tracking Concepts for Deep Space Missions," in *Free-Space Laser Communication Technologies XI*, G. Stephen Mecherle, ed., Proc. SPIE **3615**, 230–249 (1999).
7. A. Gibson, "Laser Pointing Technology," in *Laser Weapons Technology*, T.D. Steiner and P.H. Merritt, eds., Proc. SPIE **4034**, 165–174 (2000).
8. P.F. McManamon, T.A. Dorschner, D.L. Corkum, L.J. Friedman, D.S. Hobbs, M. Holz, S. Lieberman, H.Q. Nguyen, D.P. Resler, R.C. Sharp, and E.A. Watson, "Optical Phased Array Technology," Proc. of the IEEE **84**, 268–297 (1996).
9. E.A. Watson, P.F. McManamon, L.J. Barnes, and A.J. Carney, "Application of Dynamic Gratings and to Broad Spectral Band Beam Steering," in *Laser Beam Propagation and Control*, H. Weichel and L.F. Desandre, eds., Proc. SPIE **2120**, 178–185 (1994).
10. D.P. Resler, D.S. Hobbs, R.C. Sharp, L.J. Friedman, and T.A. Dorschner, "High-Efficiency Liquid-Crystal Optical Phased-Array Beam Steering," Opt. Lett. **21**, 689–691 (1996).
11. M.T. Gruneisen, T. Martinez, and D.L. Lubin, "Dynamic Holography for High-Dynamic-Range Two-Dimensional Laser Wavefront Control," in *High-Resolution Wavefront Control: Methods, Devices, and Applications III*, J.D. Gonglewski, M.A. Vorontsov, and M.T. Gruneisen, eds., Proc. SPIE **4493**, High-Resolution Wavefront Control: Methods, Devices, and Applications, San Diego, CA., Aug. 1–3 (2001).
12. M. Born and E. Wolf, *Principles of Optics*, 6th Edition (Cambridge University Press, Cambridge 1997).
13. C.M. Titus, *Refractive and Diffractive Liquid Crystal Beam Steering Devices*, Kent State Univ. Dissertation (2000).
14. J.D. Zook, "Light Beam Deflector Performance: a Comparative Analysis," Appl. Opt. **13**, 875–887 (1974).
15. "Computational Electrodynamics, The Finite Difference Time Domain Method," by A. Taflove, published by Artech House (1995).
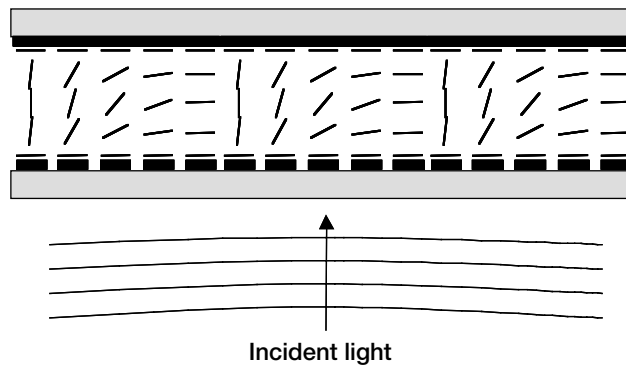
Incident light

Figure 1.—Approximate appearance of the director config-
uration of three periods from a liquid crystal spatial phase
modulator, with lower electrode voltages selected to
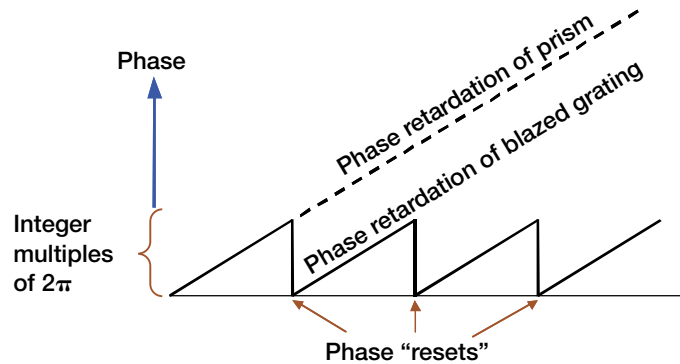produce blaze-phase grating.

Figure 2.—Ideal linear phase ramp, characteristic of deflected
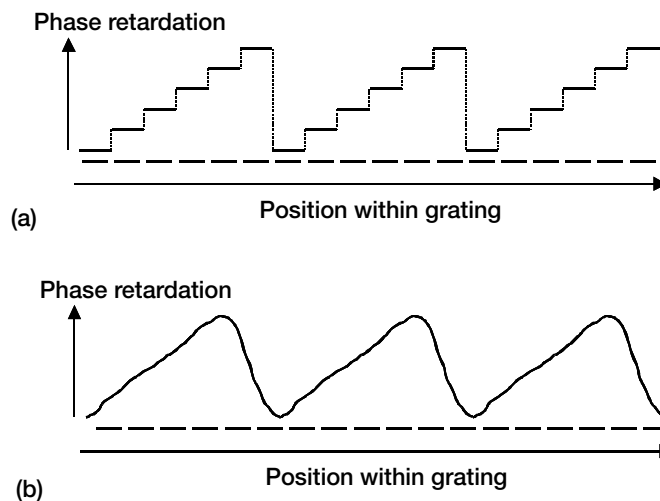plane waves, with its 2π phase degeneracies removed.

(a)

(b)

Figure 3.—Phase retardation profiles produced by (a) large
pixel stepping, and (b) small pixel OPA, showing evidence
of "phase smoothing" resulting from increased significance
of the spatial extent of fringing fields and liquid crystal
elasticity.
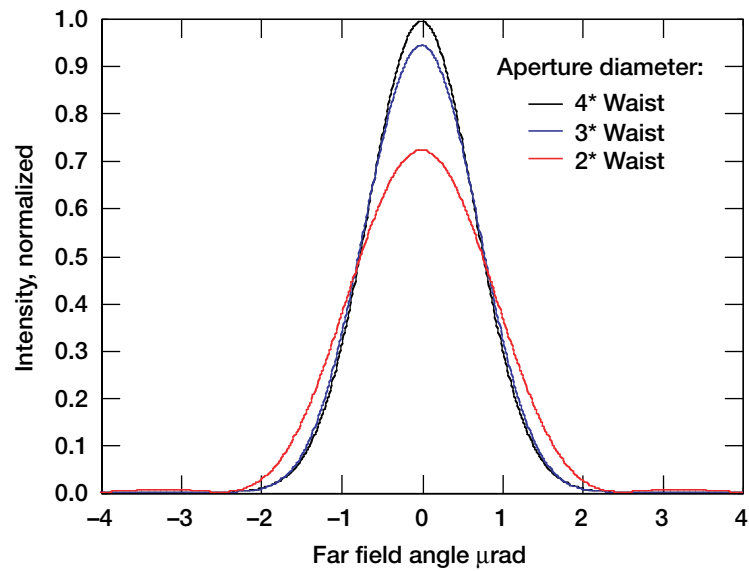
Figure 4.—Intensity profiles, in the far field, of a Gaussian beam which has been truncated in the plane of the minimum waist by an aperture. Intensity is normalized to that of an unhindered beam.
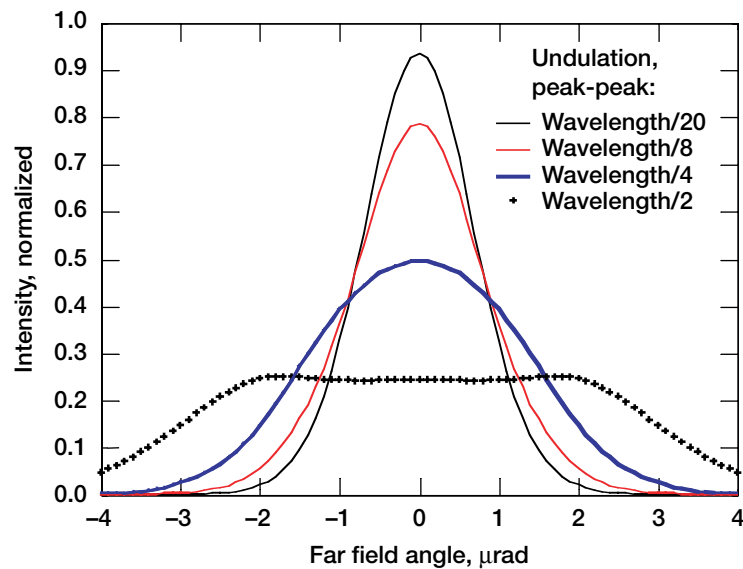
Figure 5.—Effect of sinusoidal surface undulations on far field intensity distribution of Gaussian beam reflected from a non-ideal mirror surface. Intensity is normalized to that of an unhindered beam.
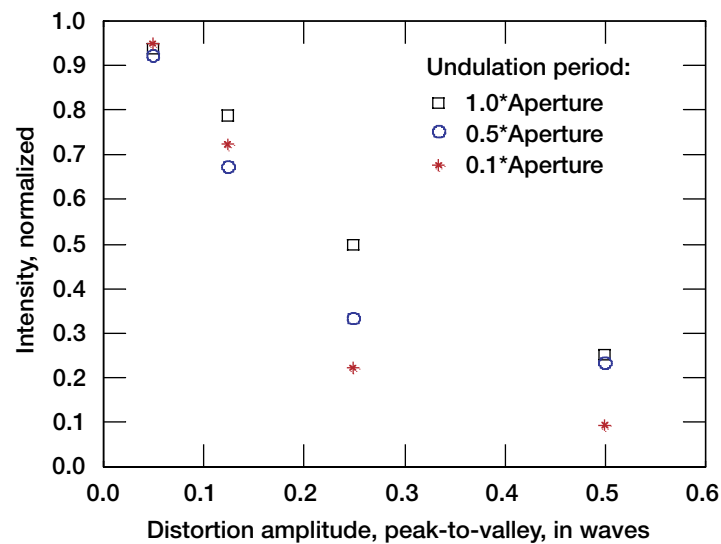
Figure 6.—Strehl ratio versus surface undulation amplitude, for 3 different undulation spatial frequencies, for a Gaussian beam reflected from a non-ideal mirror surface.
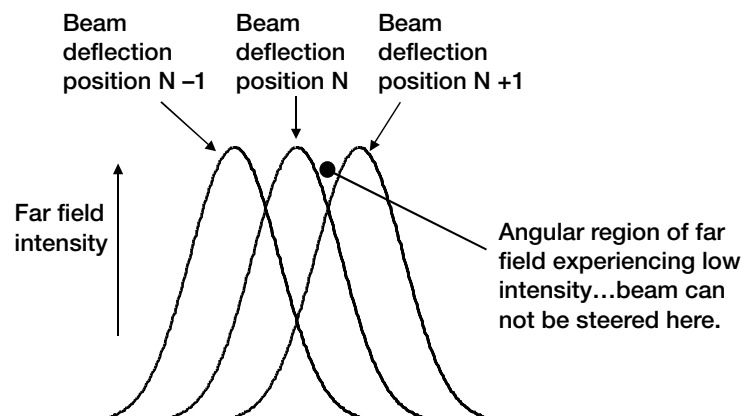
Figure 7.—Coverage of far field, from an OPA for which steering resolution is limited to the spot resolution. Not all parts of far field will be able to see the signal at its most intense.
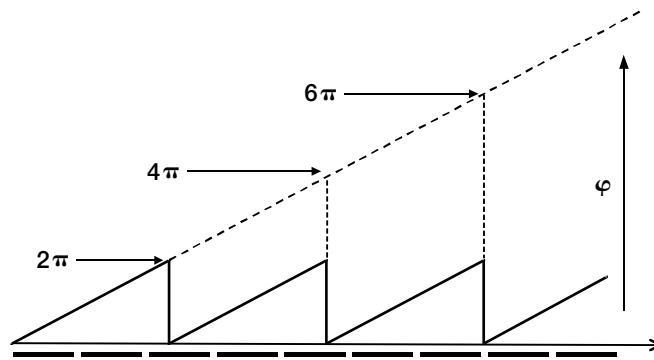
Figure 8.—Ideal linear phase ramp, after application of modulo-2π operation, overlaid onto patterned electrodes, for the case in which phase resets do not coincide with the boundary between electrodes.
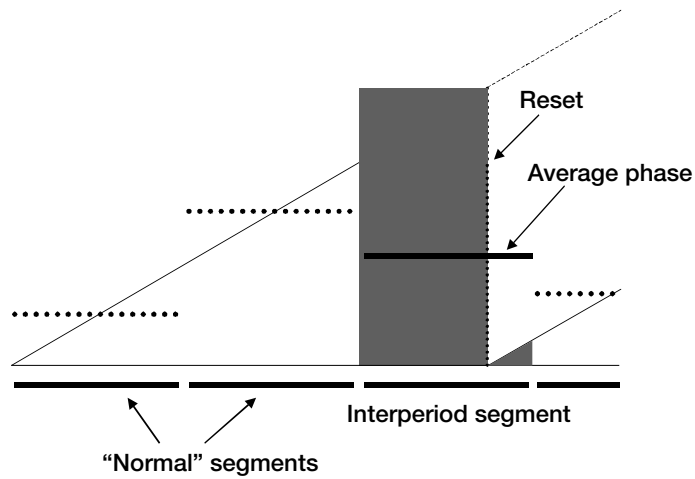
Figure 9.—For the case of Figure 7, applying the phase-averaging operation to the interperiod electrode, after first applying the modulo-2π operation to the ideal linear phase ramp.
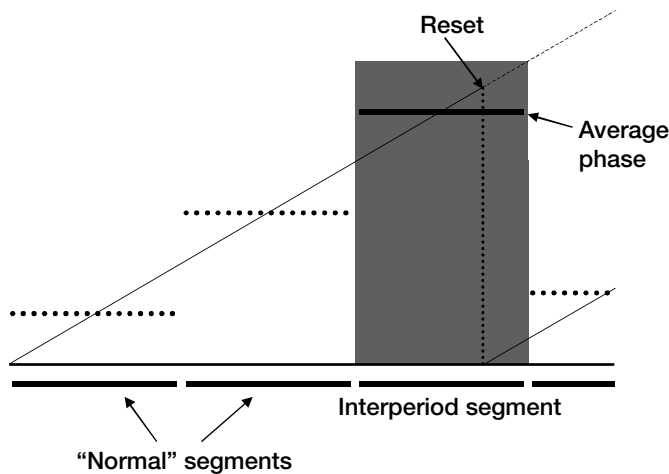

Figure 10.—For the case of Figure 7, applying the modulo-2π operation to the interperiod electrode, after first applying the phase-averaging operation to the ideal linear phase ramp.
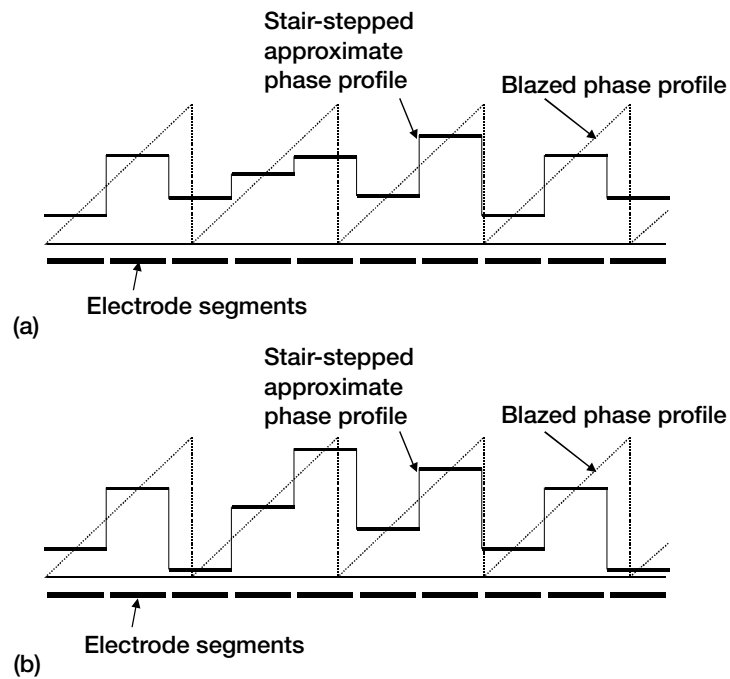
Figure 11.—Sections of grating phase profile, after (a) application of modulo-2π and then phase-averaging operation, and (b) reversing the order of those operations.
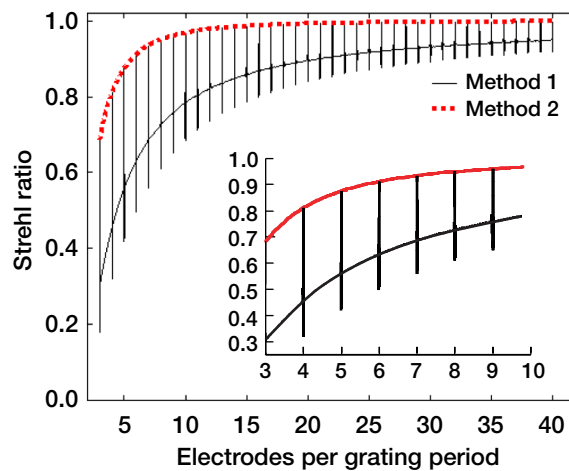

Figure 12.—Strehl ratio versus number of electrodes per ideal blaze period, showing the effects of non-integer numbers for the two methods of assigning phase to interperiod electrodes.
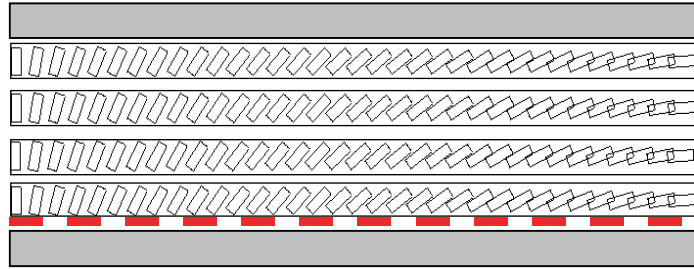
Figure 13.—Idealized configuration of liquid crystal director, providing a linearly increasing (l-r) optical path length for rays passing through the layer at normal incidence. This would constitute one period of a hypothetical liquid crystal blazed grating.
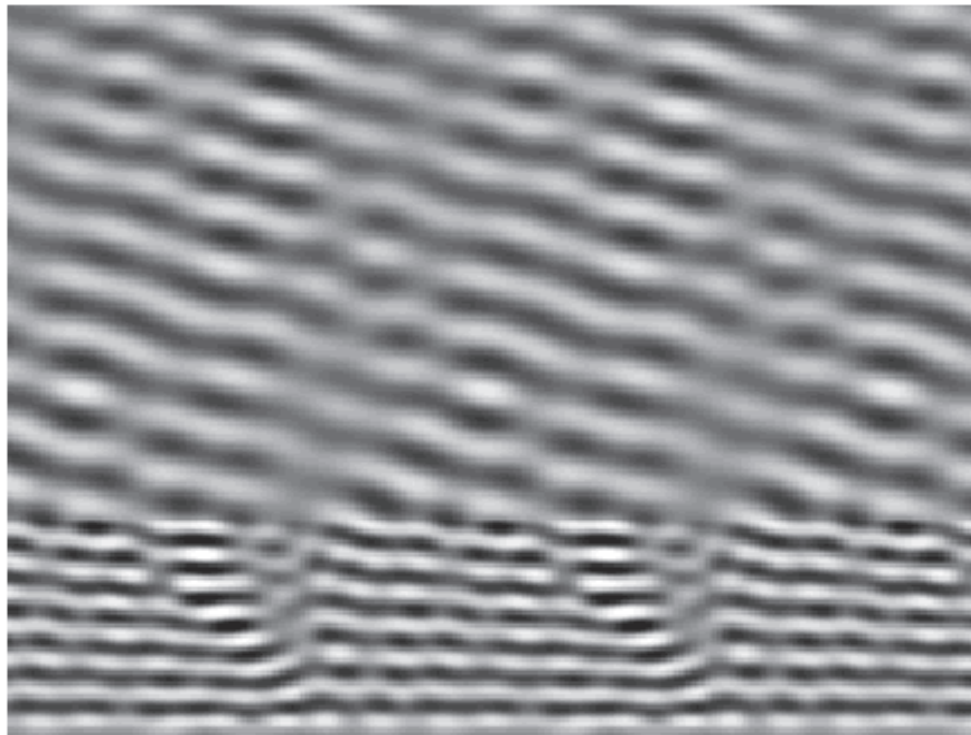

Figure 14.—Gray scale map of the transverse field propagating through and away from a section of hypothetical liquid crystal grating constructed from the building block shown in figure 13.The light is normally incident on the grating from the bottom of the figure. Approximately 3 grating periods are shown in the lower 1/3 of the picture. The upper 2/3 shows the exiting light propagating in a vacuum.
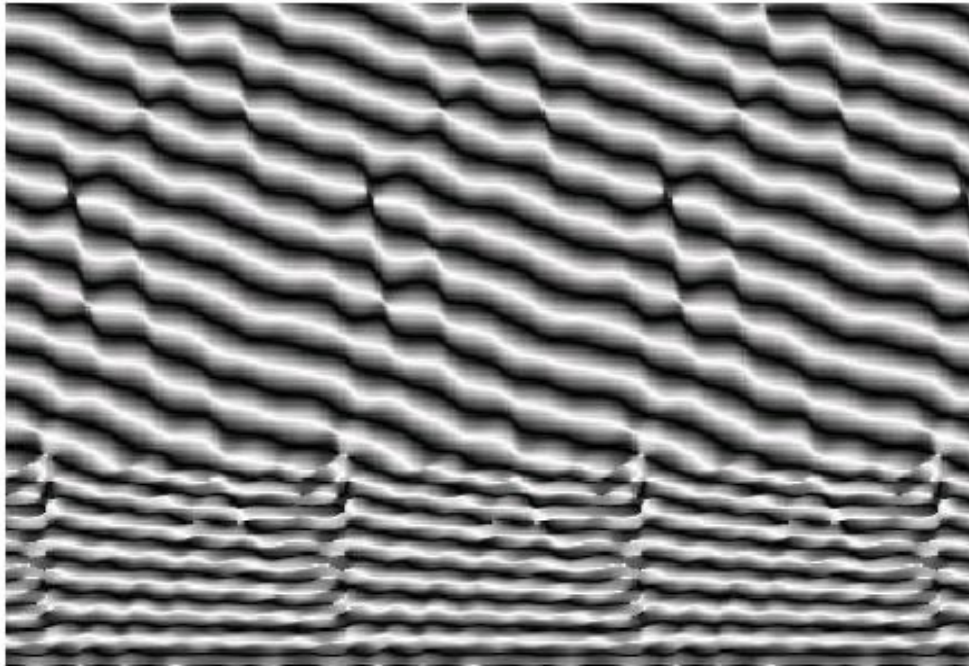
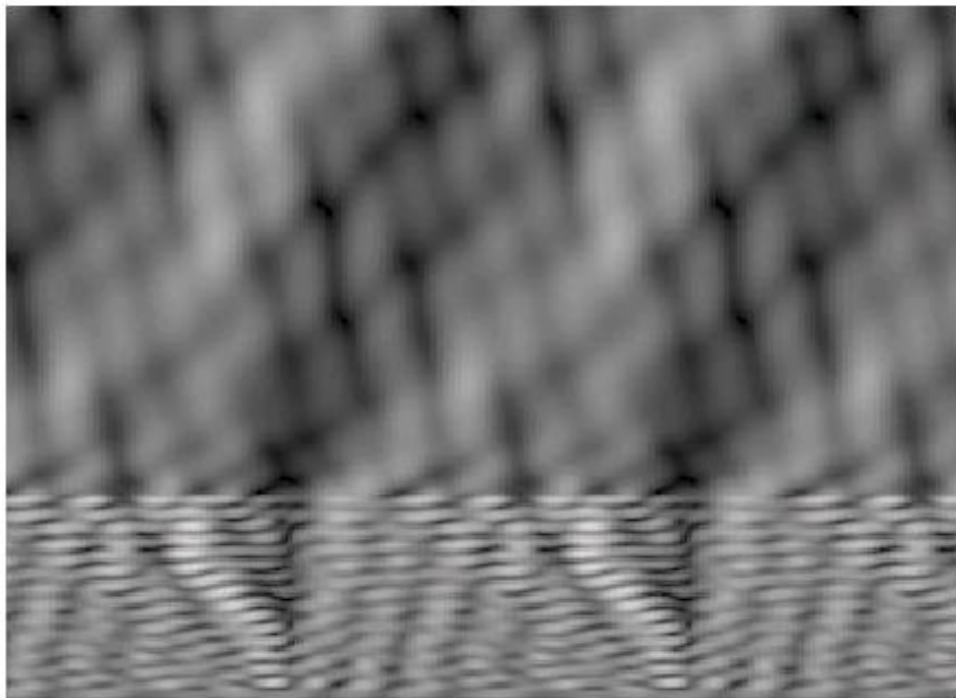Figure 15.—Similar to figure 14, but showing the phase component of the light.

Figure 16.—Similar to figure 14, but showing the intensity of the light.

REPORT DOCUMENTATION PAGE

Public reporting burden for this collection of information is estimated to average 1 hour per response, including the time for reviewing instructions, searching existing data sources, gathering and maintaining the data needed, and completing and reviewing the collection of information. Send comments regarding this burden estimate or any other aspect of this collection of information, including suggestions for reducing this burden, to Washington Headquarters Services, Directorate for Information Operations and Reports, 1215 Jefferson Davis Highway, Suite 1204, Arlington, VA 22202-4302, and to the Office of Management and Budget, Paperwork Reduction Project (0704-0188), Washington, DC 20503.

1. AGENCY USE ONLY *(Leave blank)*	2. REPORT DATE	3. REPORT TYPE AND DATES COVERED
	February 2003	Technical Memorandum

4. TITLE AND SUBTITLE

Diffraction Efficiency of Thin Film Holographic Beam Steering Devices

5. FUNDING NUMBERS

WBS–22–757–01–04

6. AUTHOR(S)

Charles M. Titus, John Pouch, Hung Nguyen, Felix Miranda, and Philip J. Bos

7. PERFORMING ORGANIZATION NAME(S) AND ADDRESS(ES)

National Aeronautics and Space Administration
John H. Glenn Research Center at Lewis Field
Cleveland, Ohio 44135–3191

8. PERFORMING ORGANIZATION REPORT NUMBER

E–13501

9. SPONSORING/MONITORING AGENCY NAME(S) AND ADDRESS(ES)

National Aeronautics and Space Administration
Washington, DC 20546–0001

10. SPONSORING/MONITORING AGENCY REPORT NUMBER

NASA TM—2003-211806

11. SUPPLEMENTARY NOTES

Prepared for the 47th Annual Meeting, International Symposium on Optical Science and Technology sponsored by the International Society for Optical Engineering, Seattle, Washington, July 7–11, 2002. Charles M. Titus and Philip J. Bos, Liquid Crystal Institute, Kent State University, Kent, Ohio 44242. John Pouch, Hung Nguyen, and Felix Miranda, NASA Glenn Research Center. Responsible person, John Pouch, organization code 5640, 216–433–3523.

12a. DISTRIBUTION/AVAILABILITY STATEMENT

Unclassified - Unlimited
Subject Category: 74   Distribution: Nonstandard

Available electronically at http://gltrs.grc.nasa.gov

This publication is available from the NASA Center for AeroSpace Information, 301–621–0390.

12b. DISTRIBUTION CODE

13. ABSTRACT *(Maximum 200 words)*

Dynamic holography has been demonstrated as a method for correcting aberrations in space deployable optics, and can also be used to achieve high-resolution beam steering in the same environment. In this paper, we consider some of the factors affecting the efficiency of these devices. Specifically, the effect on the efficiency of a highly collimated beam from the number of discrete phase steps per period is considered for a blazed thin film beam steering grating. The effect of the number of discrete phase steps per period on steering resolution is also considered. We also present some result of Finite-Difference Time-Domain (FDTD) calculations of light propagating through liquid crystal "blazed" gratings. Liquid crystal gratings are shown to spatially modulate both the phase and amplitude of the propagating light.

14. SUBJECT TERMS

Thin film; Beam steering device; Diffraction grating; Phase grating; Liquid crystal spatial light modulator; Optical simulation

15. NUMBER OF PAGES

21

16. PRICE CODE

17. SECURITY CLASSIFICATION OF REPORT	18. SECURITY CLASSIFICATION OF THIS PAGE	19. SECURITY CLASSIFICATION OF ABSTRACT	20. LIMITATION OF ABSTRACT
Unclassified	Unclassified	Unclassified	